Software Requirements Specifications (SRS) STEM Moiré GPA

Alexandre Pofelski

macid: pofelska

github: slimpotatoes

October 21, 2017

Contents

1 Revision History

Table 1: **Revision History**

Date	Version	Notes
4/10/2017	1.0	First Draft
17/10/2017	1.1	Significant corrections addressing comments and mistakes
18/10/2017	1.2	Modification of IM 3 algorithm considered not enough precise

2 Reference Material

2.1 Table of Units

Throughout this document SI (Système Internationale d'Unités) is employed as the unit system. In addition to the basic units, several derived units are used as described below. For each unit, the symbol is given followed by a description of the unit and the SI name.

Symbol	Base quantity	Name SI
m	length	metre
m^{-1}	reciprocal meter	wave number

2.2 Table of Symbols

The table that follows summarizes the symbols used in this document along with their units if applicable.

Symbol	Unit	Description
$\mathcal{B}$		2D orthonormal base
$\mathcal{C}$		Ceiling function
δ		Dirac delta function
$\Delta\overrightarrow{g_j}^{M_{\exp}}$	nm^{-1}	Variation of the jth Moiré wave vector of $SMH_{\exp}$
$\Delta\overrightarrow{g_j}^{C_{\exp}}$	nm^{-1}	Variation of the jth crystalline wave vector of $SMH_{\exp}$
ε		Strain tensor
ε_{xx}		Uniaxial strain component along $\vec{u_x}$
ε_{yy}		Uniaxial strain component along $\vec{u_y}$
ε_{xy}		Shear strain component in base $\mathcal{B}$
$\mathcal{FT}$		Fourier transform
Γ		Spatial frequency range
$\overrightarrow{g_j}$	nm^{-1}	j^{th} wave vector
g_{j_x}	nm^{-1}	Component of the jth wave vector along $\vec{u_x}$
g_{j_y}	nm^{-1}	Component of the jth wave vector along $\vec{u_y}$
$\overrightarrow{g_j}^{C}$	nm^{-1}	j^{th} crystalline wave vector
$\overrightarrow{g_j}^{C_{\text{ref}}}$	nm^{-1}	j^{th} crystalline wave vector of $I_{C_{\text{ref}}}$
$\overrightarrow{g_j}^{C_{\exp}}$	nm^{-1}	j^{th} crystalline wave vector of $SMH_{\exp}$
$\overrightarrow{g_j}^{C_{\exp}}_{\text{uns}}$	nm^{-1}	j^{th} crystalline wave vector of $SMH_{\exp}$ at its unstrained state
$\overrightarrow{g_j}^{M_{\exp}}$	nm^{-1}	j^{th} Moiré wave vector of $SMH_{\exp}$
$\overrightarrow{g_j}^{M_{\exp}}_{\text{uns}}$	nm^{-1}	j^{th} Moiré wave vector of $SMH_{\exp}$ at its unstrained state

Symbol	Unit	Description
i		Imaginary unit
I		Intensity (or number of counts)
$\mathbb{I}$		Sub-set of $\mathbb{R}$ representing the position of the pixels in an image
$I_{C_{\mathrm{ref}}}$		2D array representing the reference crystal structure
$I_{SMH_{\mathrm{exp}}}$		2D array representing the experimental SMH
$I_{SMH_{\mathrm{sim}}}$		2D array representing the simulated SMH
$I_{\varepsilon_{xx}}$		2D array representing the uniaxial strain component along $\vec{u_x}$
$I_{\varepsilon_{yy}}$		2D array representing the uniaxial strain component along $\vec{u_y}$
$I_{\varepsilon_{xy}}$		2D array representing the shear strain component in base $\mathcal{B}$
$I_{\omega_{xy}}$		2D array representing the rotation component in base $\mathcal{B}$
M_j		Mask function in Fourier space including the jth wave vector
$\mathbb{N}$		Set of natural numbers
∇		Gradient operator
∇u		Displacement gradient tensor
$\vec{\nu}$	nm^{-1}	Vector position in Fourier space
ω		Rotation tensor
O		Origin of the coordinate system
ω_{xy}	rad	Rotation element of the rotation tensor
p	nm	Pixel size
$P_{\overrightarrow{X}}$	rad	2D array representing $2\pi\overrightarrow{X}\cdot\vec{r}$
$\overrightarrow{q_{n_j,m_j}}$		Sampling vector $\vec{q}\in Q$ of couple (n_j,m_j)
Q		Set such that $Q=\{\forall(n,m)\in\mathbb{Z}^2,\vec{q}=n\vec{u_x}+m\vec{u_y}\}$
$\vec{r}$	nm	Vector position
$\mathbb{R}$		Set of real numbers
$\overrightarrow{rot}$		Curl operator
SMH_{exp}		2D array representing the experimental STEM Moiré Hologram
SMH_{sim}		2D array representing the simulated STEM Moiré Hologram
$\vec{u_x}$		Unitary vector from base $\mathcal{B}$
$\vec{u_y}$		Unitary vector from base $\mathcal{B}$
$\wedge$		Mathematical symbol for "and"
$\bigwedge$		Cross product operator
$\mathbb{Z}$		Set of integer numbers

2.3 Abbreviations and Acronyms

symbol	description
A	Assumption
AU	Arbitrary Unit
DC	Data Constraint
DD	Data Definition
EM	Electron Micrograph
GD	General Definition
GPA	Geometrical Phase Analysis
GS	Goal Statement
IM	Instance Model
LC	Likely Change
PS	Physical System Description
NR	Non functional Requirement
R	Requirement
SMH	STEM Moiré Hologram
SRS	Software Requirements Specification
STEM	Scanning Transmission Electron Microscopy
T	Theoretical Model

3 Introduction

3.1 Purpose of Document

The purpose of the document is to provide a detailed description of the functional and the non-functional requirements of the STEM Moiré GPA software. The theoretical models on which the requirements are based on are also described to provide the context of each instance model.

3.2 Scope of Requirements

The scope of requirements are limited to the realization of GS 1 which corresponds to transform a certain type of data to another one based on multiple user inputs. STEM Moiré GPA is for the moment limited to the study of mono-crystalline material undergoing a relative small deformation with respect to its unstrained state.

3.3 Characteristics of Intended Reader

The intended reader is expected to have a minimum knowledge in mathematics at undergraduate level. Simplification of some physical concepts are proposed to make the document technically accessible. Nevertheless, a basic knowledge in Transmission Electron Microscopy, electron/matter interaction and elastic strain theory is recommended to get a deeper understanding of the document.

3.4 Organization of Document

The document follows the template of the SRS document proposed by [1, 2].

4 General System Description

This section identifies the interfaces between the system and its environment, describes the user characteristics and lists the system constraints.

4.1 System Context

STEM Moiré GPA is intended to transform specific data acquired from the microscope into physical information related to the sample analysed. The variety of samples is potentially huge therefore to cover the maximum of cases, multiple interactions with the user are required to process the data correctly. Responsibilities between the user and the STEM Moiré GPA are described as follows:

- User Responsibilities:

- Provide the minimum information required by the STEM Moiré GPA software.
- Use the software in the limits it is intended to by respecting A 4, A 5, A 6 and A 7.
- Be aware of the potential effects of user inputs on the quality of the final data.
- Judge the correctness of the data.
- Be particularly cautious on the use of the final data quantitatively. The quantitative aspect cannot be fully uncorrelated from the user inputs.
- Use a pointing device, a keyboard and a display to interface with STEM Moiré GPA.

- STEM Moiré GPA Responsibilities:

  - Inform the user of their responsibilities in using STEM Moiré GPA.
  - Preserve the integrity of original data and not add any hidden processing steps on the final data such as, but not limited to, smoothing, blurring, averaging, de-noising and binning.
  - Inform user of wrong format or missing information regarding the inputs.
  - Inform the user of a potential insufficient quality of the final results which could lead to non reliable physical interpretations.

4.2 User Characteristics

The end user of STEM Moiré GPA should have a relative strong background in Physics (interaction electron/matter) and Mathematics (or signal processing) at graduate level to get a reliable sense of the data processed. The multiple interactions between the user and STEM Moiré GPA have significant impact on the final results which can lead to some physical misinterpretations. Basic practical and theoretical knowledge in Electron Microscopy is recommended because of the terminology used in the document.

4.3 System Constraints

To be considered by the electron microscopy community, STEM Moiré GPA has to be able to read dm3 files format, an non-standard format used by the electron detector manufacturer.

5 Specific System Description

5.1 Problem Description

STEM Moiré GPA project is a software capable of converting a STEM Moiré hologram into 2D relative strain maps. Terminologies and the physical system are described below.

5.1.1 Terminology and Definitions

Regarding the complexity of the electron/matter interaction, some crude simplifications are proposed to describe the terminologies below. While sometimes not realistic, the simplifications should help in visualizing the context and the type of data the STEM Moiré GPA software is subjected to. Nevertheless, all the simplifications proposed are not affecting the definition of the concept used at the software level.

- **2D Cartesian coordinate system**: orthonormal coordinate system model by the base $\mathcal{B} = (O, \vec{u_x}, \vec{u_y})$ with O representing the origin and M a point with coordinate the (x, y), such that any vector $\vec{r} = \overrightarrow{OM}$ can be expressed as the following :

$$\forall (x, y) \in \mathbb{R}^2, \vec{r} = x\vec{u_x} + y\vec{u_y} \tag{1}$$

- **Pixel**: smallest addressable element sampling a 2D continuum.

- **Detector**: Element in fig. 1 collecting and counting the electron that crossed the sample.

- **Electron Micrograph (EM)**: 2D array collected in an electron microscope representing the number of electron crossing the sample (intensity) at each pixel location.

- **Scanning grid**: set representing the succession of the STEM probe positions when collecting the STEM EM. Equivalently the scanning grid represents the relative position of the pixel with respect to the sample when acquiring the EM. A simplified version of the STEM EM formation can be visualized in fig. 1. The positions of the STEM probe are located at the intersection of the black grid lines.
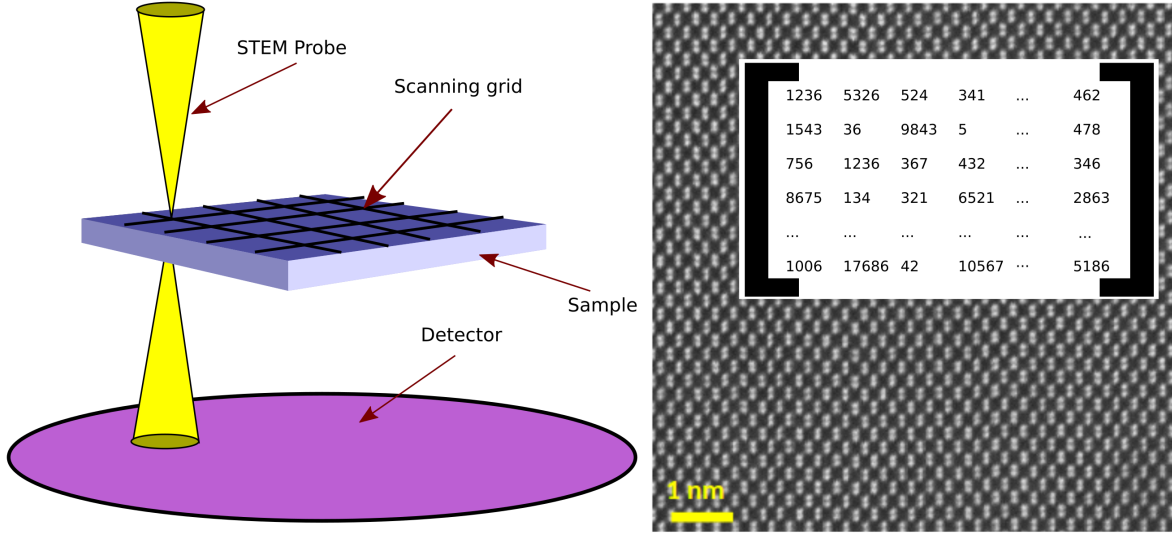
Figure 1: (Left) Schematic of the STEM EM formation with the STEM probe scanning the sample at each intersection of the grid lines. The electrons crossing the sample are collected on the detector and counted during the acquisition time. (Right) STEM EM on a pure silicon sample revealing its atomic structure. In the inset is highlighted the type of data the STEM EM corresponds to which is a 2D array with the intensity collected on each pixel.

- **Hologram**: Result from an interference between two or multiples waves.
  Let consider two monochromatic plane waves ψ_1 and ψ_2 with their respective amplitude A_j, phase ϕ_j and wave vector $\vec{k}_j$ in the 2D Cartesian system interfering with each other. The resulting hologram ψ_H can be modelled as follows with :

$$\forall (x,y) \in \mathbb{R}^2, \psi_H(\vec{r}) = \psi_1 + \psi_2 = A_1 e^{i(\vec{k_1}\cdot\vec{r})+i\phi_1} + A_2 e^{i(\vec{k_2}\cdot\vec{r})+i\phi_2} \tag{2}$$

  The intensity I_H can be calculated as follows, with ψ_H^* representing the complex conjugate of ψ_H

$$\forall (x,y) \in \mathbb{R}^2, I_H(\vec{r}) = \psi_H \psi_H^* = A_1^2 + A_2^2 + \\ A_1 A_2 \left(e^{i(\vec{k_1}-\vec{k_2})\cdot\vec{r}+i(\phi_1-\phi_2)} + e^{i(\vec{k_2}-\vec{k_1})\cdot\vec{r}+i(\phi_2-\phi_1)} \right) \tag{3}$$

  The more waves are contributing to the hologram, the more complex eq. (3) will be. However, similar factors will appear with constants and cross product terms.

- **Moiré hologram**: Result from interference between two or multiple waves with similar but not equal wave numbers (or wave vectors in 2D).

- **Crystal lattice**: Periodic arrangement of atoms forming matter.

- **STEM Moiré hologram (SMH)**: EM collected in STEM and resulting from the Moiré interference between the scanning grid and the crystal lattice.

- **Strain map**: 2D array mapping the evolution of one element of the 2D strain or rotation tensor.

5.1.2 Physical System Description

The physical system of STEM Moiré GPA, as shown in fig. 2, includes the following elements:

- The STEM Moiré hologram as the results of the interaction between the scanning grid and the crystal periodicity of the sample.

- Physical inputs provided by the user to convert a STEM Moiré hologram into strain and rotation maps.

STEM scanning grid

Sample

STEM Moiré hologram in which the strain field from the sample is embedded

Use a reference related to the sample and simulate the hologram formation process to compare it to the experimental data

Choose first wave vector and apply GPA

Choose second wave vector and apply GPA

Convert the information from the hologram into strain information from the sample

User

Convert the information from the hologram into strain information from the sample

Select an unstrained area in the image

Select an unstrained area in the image

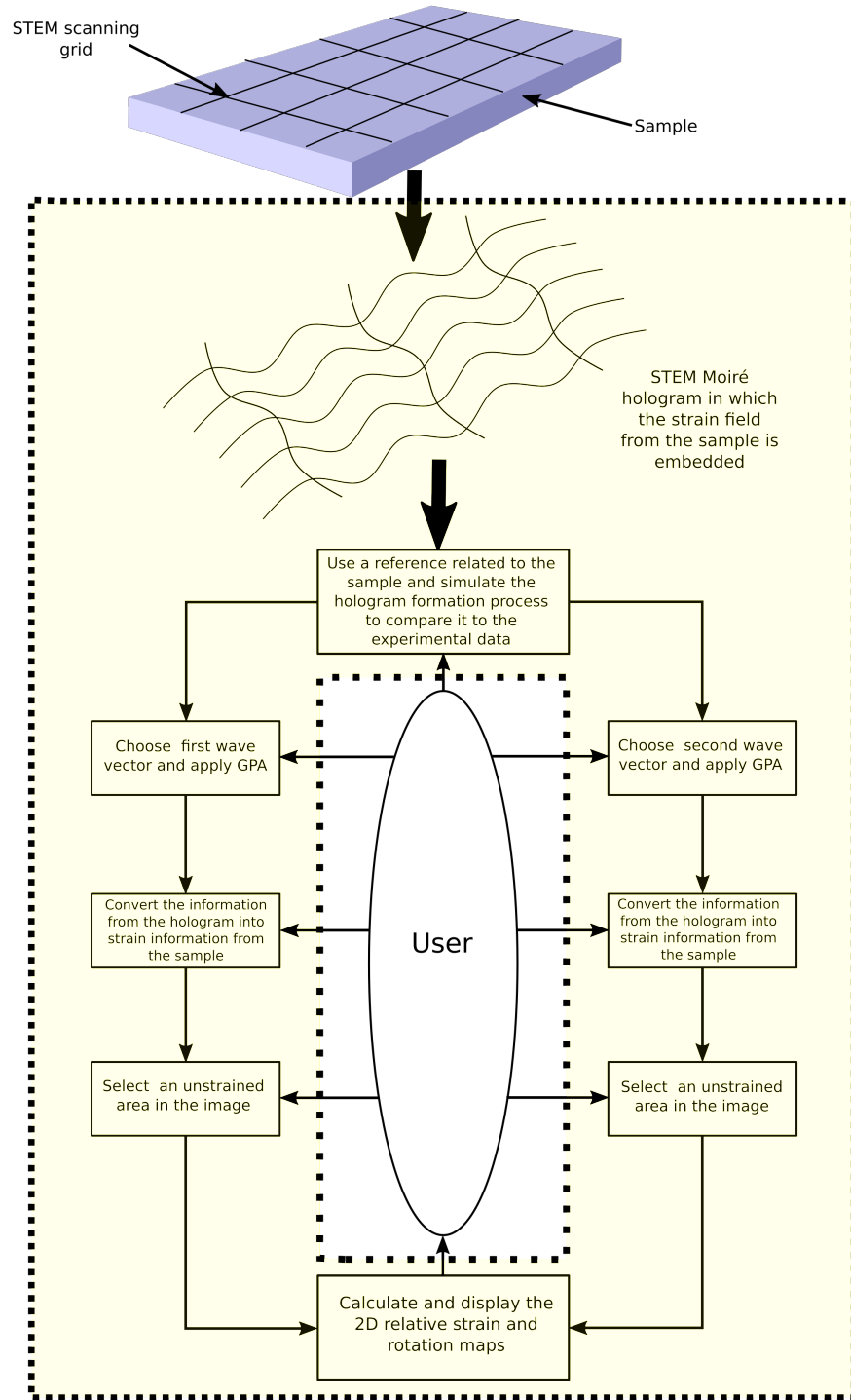Calculate and display the 2D relative strain and rotation maps

Figure 2: Physical system of STEM Moiré GPA highlighted in the yellow area.

5.1.3   Goal Statements

Given the system description, the goal statement is:

GS 1 Extract and display the relative 2D strain field from a STEM Moiré hologram.

5.2   Solution Characteristics Specification

5.2.1   Assumptions

A 1 The microscope has a limit in resolution corresponding to the probe size and thus cannot resolve any spatial frequency higher than $g_{j_{\lim}}$.

A 2 Since the STEM EM is discretized in pixels, the smallest feature detectable is composed of two pixels. Therefore, in reciprocal space, the maximum range of spatial frequency detectable is $\Gamma = [-\frac{1}{2p}, \frac{1}{2p}]^2$.

A 3 The probe size is smaller than the area covered by one pixel. Therefore, information gathered on one pixel is only provided by the area covered by the pixel (no blurring) and A 1 is the only limiting factor regarding resolution.

A 4 The gradient of the deformation field is small. Therefore,

$$\forall \vec{r} \in \mathbb{R}^2, \ \nabla(\Delta\overrightarrow{g_j} \cdot \vec{r}) = (\Delta\overrightarrow{g_j} \cdot \nabla)\vec{r} + (\vec{r} \cdot \nabla)\Delta\overrightarrow{g_j} + \Delta\overrightarrow{g_j}\bigwedge\overrightarrow{rot}(\vec{r}) + \vec{r}\bigwedge\overrightarrow{rot}(\Delta\overrightarrow{g_j}))$$
$$\forall \vec{r} \in \mathbb{R}^2, \ \nabla(\Delta\overrightarrow{g_j} \cdot \vec{r}) \approx \Delta\overrightarrow{g_j}$$

A 5 The deformation magnitude is small. Therefore, $\frac{||\Delta\overrightarrow{g_j}||}{||\overrightarrow{g_j}||} \leq 0.1$

A 6 The user knows the crystal structure of the sample analysed at its unstrained state or can provide a reference in which is embedded the crystal structure information at its unstrained state.

A 7 The sample, from which the SMH is acquired, is mono-crystalline.

5.2.2   Theoretical Models

T 1 2D periodic sampling

- <u>Equation</u>: Equation (5)

- <u>Description</u>: In the 2D Cartesian coordinate system $\mathcal{B}$, the scanning grid can be seen as sampler S sampling a continuous function f. In the context of the STEM Moiré GPA project, the sampler is set to be periodic with the same periodicity p (called pixel

size) in both x and y directions (2D Dirac comb). The resulting sampled version f_S of f can be represented as the following with δ representing the Dirac function:

$$\forall (x,y) \in \mathbb{R}^2, f_S(x,y) = S(x,y) \times f(x,y)$$

$$\forall (x,y) \in \mathbb{R}^2, f_S(x,y) = \sum_{n=-\infty}^{n=+\infty} \sum_{m=-\infty}^{m=+\infty} \delta(x - np, y - mp) \times f(x,y) \tag{4}$$

For shorter notations, it is possible to define a set Q as follows $Q = \{\forall (n,m) \in \mathbb{Z}^2, \vec{q} = n\vec{u_x} + m\vec{u_y}\}$ and thus simplify eq. (4)

$$\forall (x,y) \in \mathbb{R}^2, f_S(\vec{r}) = \sum_{q \in Q} \delta(\vec{r} - p\vec{q}) f(\vec{r}) \tag{5}$$

- Source: [3]

- Ref by: DD 2, IM 1, IM 4

T 2 <mark>**Geometrical Phase Analysis**</mark>

- Equation: Equation (9)

- Description: Let consider a function f decomposed in Fourier series as the following with

$$\forall \vec{r} = (x_1, ..., x_n) \in \mathbb{R}^n, f(\vec{r}) = \sum_{j=-\infty}^{j=+\infty} C_j e^{i(\vec{k_j} \cdot \vec{r})}$$

$$\forall \vec{r} = (x_1, ..., x_n) \in \mathbb{R}^n, f(\vec{r}) = \sum_{j=-\infty}^{j=+\infty} A_j e^{i((\vec{k_j} \cdot \vec{r}) + B_j)} \tag{6}$$

If there is a small perturbation locally of the n-dimensions wave vector $\vec{k_j}$, it is possible to model it by allowing B_j to be a function of $\vec{r}$.

$$\forall \vec{r} = (x_1, ..., x_n) \in \mathbb{R}^n, f(\vec{r}) = \sum_{j=-\infty}^{j=+\infty} A_j e^{i((\vec{k_j} \cdot \vec{r}) + B_j(\vec{r}))} \tag{7}$$

The objective of GPA is to extract the perturbation (one chosen $B_j(\vec{r})$) from f in Fourier space. Let's consider $\widetilde{f}$ the Fourier transform of f such that

$$\forall \vec{\nu} = (\nu_1, ..., \nu_n) \in \mathbb{R}^n, \forall \vec{r} = (x_1, ..., x_n) \in \mathbb{R}^n, \widetilde{f}(\vec{\nu}) = \mathcal{FT}(f(\vec{r}))$$

$$\forall \vec{\nu} = (\nu_1, ..., \nu_n) \in \mathbb{R}^n, \forall \vec{r} = (x_1, ..., x_n) \in \mathbb{R}^n, \widetilde{f}(\vec{\nu}) = \sum_{j=-\infty}^{j=+\infty} \mathcal{FT}(C_j(\vec{r}) \times e^{i(\vec{k_j} \cdot \vec{r})})$$

$$\forall \vec{\nu} \in \mathbb{R}^n, \widetilde{f}(\vec{\nu}) = \sum_{j=-\infty}^{j=+\infty} \widetilde{C_j}(\vec{\nu}) * \delta(\vec{\nu} - \vec{k_j})$$

$$\forall \vec{\nu} \in \mathbb{R}^n, \widetilde{f}(\vec{\nu}) = \sum_{j=-\infty}^{j=+\infty} \widetilde{C_j}(\vec{\nu} - \vec{k_j})$$

(8)

If all the $\vec{k_j}$ are separated enough to be isolated with a mask, then $B_j(\vec{r})$ can be extracted by considering the inverse Fourier transform of the masked area and expressing the result in term of amplitude and phase. In mathematical formalism, $B_j(\vec{r})$ is extracted as follows with $\mathcal{G} = ([\nu_1^D, \nu_1^U], ..., [\nu_n^D, \nu_n^U])$ and ν_i^D, ν_i^U two real numbers defining respectively the lower and the upper side of the interval $[\nu_i^D, \nu_i^U]$.

$$\text{if } \exists \, M : \left| \begin{array}{ccc} \mathbb{R}^n & \longrightarrow & \mathbb{C} \\ \vec{\nu} & \longmapsto & M(\vec{\nu}) \end{array} \right. \Big/ \begin{cases} M(\vec{\nu} - \vec{k_j})\widetilde{f}(\vec{\nu}) = \widetilde{C_j}(\vec{\nu} - \vec{k_j}) & \text{for } \vec{\nu} \in \mathcal{G} \\ M(\vec{\nu} - \vec{k_j})\widetilde{f}(\vec{\nu}) = 0 & \text{for } \vec{\nu} \notin \mathcal{G} \end{cases}$$

$$\Rightarrow \begin{array}{l} |\mathcal{FT}^{-1}[M(\vec{\nu})\widetilde{f}(\vec{\nu} + \vec{k_j})]| = |\mathcal{FT}^{-1}[\widetilde{C}(\vec{\nu})]| = A_j \\ arg(\mathcal{FT}^{-1}[M(\vec{\nu})\widetilde{f}(\vec{\nu} + \vec{k_j})]) = arg(\mathcal{FT}^{-1}[\widetilde{C}(\vec{\nu})]) = B_j(\vec{r}) \end{array}$$

(9)

- Source: [4,5]

- Ref by: DD 1, IM 2

Description of the GPA method in a 1D coordinate system

Let's consider a function f such that

$$\forall x \in \mathbb{R}, f(x) = C_0 e^{i(k_0 x)} + C_1 e^{i(k_1 x)}$$

Let's consider a small perturbation of k_1 modelled as the following

$$\forall x \in \mathbb{R}, f(x) = C_0 e^{i(k_0 x)} + A_1 e^{i(k_1 x) + i B_1(x)}$$

Applying the GPA method on f,

$$\forall \nu \in \mathbb{R}, \widetilde{f}(\nu) = C_0 \delta(\nu - k_0) + \widetilde{C_1}(\nu) * \delta(\nu - k_1)$$
$$\forall \nu \in \mathbb{R}, \widetilde{f}(\nu) = C_0 \delta(\nu - k_0) + \widetilde{C_1}(\nu - k_1)$$

Considering the perturbation around k_1 to be small and that k_0 and k_1 are enough separated such that the perturbation is located around k_1 in frequency space, it is possible to define a mask M and constant $\epsilon \in \mathbb{R}$ such that:

$$\forall \nu \in \mathbb{R}, M(\nu) = \begin{cases} 1 & \text{for } \nu - k_1 \in [-\epsilon, +\epsilon] \, / \, k_0 \notin [k_1 - \epsilon, k_1 + \epsilon] \\ 0 \end{cases}$$

In such case, multiply the mask M with the Fourier transform of f isolates $\widetilde{C_1}$ from the sum and can be independently transformed as follows:

$$\forall \nu \in \mathbb{R}, M(\nu - k_1)\widetilde{f}(\nu) = \widetilde{C_1}(\nu - k_1)$$

Setting, $\lambda = \nu - k_1$ and performing the inverse Fourier transform of the masked Fourier transform of f, the perturbation can be extracted.

$$\forall \nu \in \mathbb{R}, M(\lambda)\widetilde{f}(\lambda + k_1) = \widetilde{C_1}(\lambda)$$
$$\forall x \in \mathbb{R}, \mathcal{FT}^{-1}[M(\lambda)\widetilde{f}(\lambda + k_1)] = C_1(x)$$
$$\Rightarrow \begin{cases} |C_1(x)| = A_1 \\ arg(C_1(x)) = B_1(x) \end{cases}$$

T 3 <mark>**Strain decomposition model**</mark>

- <u>Equation</u>: Equation (10)

- <u>Description</u>: In infinitesimal strain theory with small displacement and small gradient of displacement (A 4, A 5), the displacement gradient tensor ∇u can be decomposed in two independent tensors: the symmetric strain tensor ε and the anti-symmetric rotation tensor ω. Their relationship can be described as follows:

$$
\begin{aligned}
\nabla u = \varepsilon + \omega &= \begin{bmatrix} \varepsilon_{xx} & \varepsilon_{xy} \\ \varepsilon_{xy} & \varepsilon_{yy} \end{bmatrix} + \begin{bmatrix} 0 & \omega_{xy} \\ -\omega_{xy} & 0 \end{bmatrix} \\
\varepsilon &= \frac{1}{2}(\nabla u + (\nabla u)^T) \\
\omega &= \frac{1}{2}(\nabla u - (\nabla u)^T)
\end{aligned}
\tag{10}
$$

- <u>Source</u>: [4,5]

- <u>Ref by</u>: DD 3, IM 3, IM 5

5.2.3 General Definitions

No general definitions are needed for the current documentation.

5.2.4 Data Definitions

DD 1 <mark>**Variation of the crystalline wave vector $\Delta\overrightarrow{g_j}$ (strain in crystal lattice)**</mark>

- ⋆ <u>Equation</u>: Equation (13)

⋆ Description: For the purpose of the STEM Moiré GPA, only mono-crystalline samples are analysed (A 7). In the case of a perfect periodic atomic arrangement, the crystalline lattice I_c can be described in Fourier series with C_j the complex Fourier coefficient related to the crystalline wave vector $\vec{g_j}$ in the 2D Cartesian system $\mathcal{B}$.

$$\forall (x,y) \in \mathbb{R}^2, I_C(\vec{r}) = \sum_{j=-\infty}^{j=+\infty} C_j e^{i(\vec{g_j} \cdot \vec{r})} \tag{11}$$

If the crystal is deformed, the relative position of the atoms will be slightly modified from their original unstrained configuration. The local deformation is breaking locally the perfect periodicity of the crystalline lattice. In the case of small deformation (A 5), C_j can be allowed to vary in space in eq. (11). Representing C_j with a phase A_j and an amplitude P_j, a pure displacement is only contributing in the phase component. The strain information is therefore embedded in $P_{g_j}(\vec{r})$ such that $P_{g_j}(\vec{r}) = 2\pi \Delta \vec{g_j}(\vec{r}) \cdot \vec{r}$ where $\Delta \vec{g_j}$ represent the variation of the crystalline vector compared to its unstrained state.

$$\forall (x,y) \in \mathbb{R}^2, I_C(\vec{r}) = \sum_{j=-\infty}^{j=+\infty} C_j(\vec{r}) e^{i(\vec{g_j} \cdot \vec{r})}$$
$$\forall (x,y) \in \mathbb{R}^2, I_C(\vec{r}) = \sum_{j=-\infty}^{j=+\infty} A_j e^{i(\vec{g_j} \cdot \vec{r}) + i P_{g_j}(\vec{r})} \tag{12}$$

By applying GPA (T 2) on eq. (12), $P_{g_j}(\vec{r})$ can be extracted. Then by applying A 4, the gradient ∇ of $P_{g_j}(\vec{r})$ can be approximate as follows

$$\nabla P_{g_j}(\vec{r}) = 2\pi [\nabla (\Delta \vec{g_j} \cdot \vec{r})] \approx 2\pi \Delta \vec{g_j}(\vec{r}) \tag{13}$$

⋆ Source: [4]

⋆ Ref by: T 2, IM 3, IM 5

DD 2 STEM Moiré hologram I_{SMH}

⋆ Equation: Equation (20)

⋆ Description: Combining eq. (12) and eq. (4), a STEM Moiré hologram I_{SMH} can be described as follows

$$\forall (x,y) \in \mathbb{R}^2, I_{SMH}(\vec{r}) = \sum_{q \in Q} \delta(\vec{r} - p\vec{q}) \times \sum_{j=-\infty}^{j=+\infty} A_j e^{i(\vec{g_j} \cdot \vec{r}) + i P_{g_j}(\vec{r})} \tag{14}$$

Equation (14) corresponds physically to the 2D sampling of a 2D periodic crystalline structure. By modifying p the scanning periodicity (or the pixel size), it is possible to

11

adjust the spatial frequency of the SMH. Applying A 1 and A 3, the expression of I_C in eq. (12) is simplified since the series becomes a finite sum.

$$\forall (x,y) \in \mathbb{R}^2, I_C(\vec{r}) = \sum_{j=-j_{lim}}^{j=+j_{lim}} A_j e^{i(\vec{g_j} \cdot \vec{r}) + iP_{g_j}(\vec{r})} \tag{15}$$

Therefore, the STEM Moiré hologram I_{SMH} is also simplified as follows:

$$\forall (x,y) \in \mathbb{R}^2, I_{SMH}(\vec{r}) = \sum_{q \in Q} \delta(\vec{r} - p\vec{q}) \times \sum_{j=-j_{lim}}^{j=+j_{lim}} A_j e^{i(\vec{g_j} \cdot \vec{r}) + iP_{g_j}(\vec{r})} \tag{16}$$

Calculating $\widetilde{I}_{SMH}$ the Fourier transform of I_{SMH}, it is possible to notice that $\widetilde{I}_{SMH}$ is $(1/p, 1/p)$ periodic.

$$\forall (\nu_x, \nu_y) \in \mathbb{R}^2, \widetilde{I}_{SMH}(\nu_x, \nu_y) = \frac{1}{p^2} \sum_{n=-\infty}^{n=+\infty} \sum_{m=-\infty}^{m=+\infty} \delta(\nu_x - \frac{n}{p}, \nu_y - \frac{m}{p}) * \widetilde{I}_C(\nu_x, \nu_y)$$

$$\forall (\nu_x, \nu_y) \in \mathbb{R}^2, \widetilde{I}_{SMH}(\nu_x, \nu_y) = \frac{1}{p^2} \sum_{n=-\infty}^{n=+\infty} \sum_{m=-\infty}^{m=+\infty} \widetilde{I}_C(\nu_x - \frac{n}{p}, \nu_y - \frac{m}{p}) \tag{17}$$

$$\forall (\nu_x, \nu_y) \in \mathbb{R}^2, \widetilde{I}_{SMH}(\nu_x + \frac{1}{p}, \nu_y + \frac{1}{p}) = \widetilde{I}_{SMH}(\nu_x, \nu_y)$$

Therefore it is possible to restrain the calculation of $\widetilde{I}_{SMH}$ for $\vec{\nu} \in [-\frac{1}{2p}, \frac{1}{2p}]^2 = \Gamma$ and respect assumption A 2. Nevertheless, eq. (16) (or equivalently eq. (17)) has still an infinite set of terms in the sum since the set Q is not finite. Therefore, eq. (16), at this stage, is unusable. Applying A 1, it is possible to fix a condition for $\widetilde{I}_C$ as follows:

$$\forall (\nu_x, \nu_y) \notin [-g_{lim}, g_{lim}]^2, \widetilde{I}_C(\nu_x, \nu_y) = 0 \tag{18}$$

As a consequence,

$$\exists (N_{\lim}, N_{\lim}) \in \mathbb{N}^2 / \forall (\nu_x, \nu_y) \in \Gamma, \ \widetilde{I}_C(\nu_x - \frac{N_{\lim}}{p}, \nu_y - \frac{N_{\lim}}{p}) = 0 \tag{19}$$

It is possible thus to define $Q_{\lim} = \{\forall (n,m) \in \mathbb{Z}^2 \cap [-N_{\lim}, N_{\lim}]^2, \ \vec{q} = n\vec{u_x} + m\vec{u_y}\}$ and rewrite eq. (17) in a usable format with a finite number of terms in the sum, as the following:

$$\forall (\nu_x, \nu_y) \in \Gamma, \widetilde{I}_{SMH}(\nu_x, \nu_y) = \frac{1}{p^2} \sum_{n=-N_{\lim}}^{n=+N_{\lim}} \sum_{m=-N_{\lim}}^{m=+N_{\lim}} \widetilde{I}_C(\nu_x - \frac{n}{p}, \nu_y - \frac{m}{p})$$

$$\forall \vec{\nu} \in \Gamma, \widetilde{I}_{SMH}(\vec{\nu}) = \frac{1}{p^2} \sum_{\vec{q} \in Q_{\lim}} \widetilde{I}_C(\vec{\nu} - \frac{\vec{q}}{p}) \tag{20}$$

⋆ <u>Source</u>: [6]

⋆ <u>Ref by</u>: DD 1, T 1, IM 1, IM 4

From sampling to interferometry

Since the Dirac comb function is also periodic, the sampler can also be represented into Fourier series

$$\forall (x,y) \in \mathbb{R}^2, S(\vec{r}) = \sum_{q \in Q} \delta(\vec{r} - p\vec{q}) = \frac{1}{p^2} \sum_{q \in Q} e^{\frac{i}{p}\vec{q}\cdot\vec{r}} \tag{21}$$

Using eq. (21) in eq. (16), it is possible to recognize an interference equation between multiple plane waves (a more complex version of eq. (3)), justifying the terminology hologram in the sampling context.

$$\forall (x,y) \in \mathbb{R}^2, I_{SMH}(\vec{r}) = \frac{1}{p^2} \sum_{q \in Q} \sum_{j=-j_{\lim}}^{j=+j_{\lim}} A_j e^{i\vec{g_j}\cdot\vec{r} + \frac{i}{p}\vec{q}\cdot\vec{r} + iP_{g_j}(\vec{r})}$$

$$\forall (x,y) \in \mathbb{R}^2, I_{SMH}(\vec{r}) = \frac{1}{p^2} \sum_{q \in Q} \sum_{j=-j_{\lim}}^{j=+j_{\lim}} A_j e^{i(\vec{g_j} - \frac{1}{p}\vec{q})\cdot\vec{r} + iP_{g_j}(\vec{r})} \tag{22}$$

DD 3 <mark>**Deformation gradient tensor ∇u from crystalline wave vectors**</mark>

<u>Equation</u>: Equation (23)

<u>Description</u>: Let's consider $\vec{g_j} = \vec{g}_{j\,\text{uns}} + \Delta\vec{g}_j$ with $\vec{g}_{j\,\text{uns}}$ representing the crystalline wave vector at its unstrained state. If $\vec{g}_{j\,\text{uns}} = g_{j_x\,\text{uns}}\vec{u_x} + g_{j_y\,\text{uns}}\vec{u_y}$ and $\Delta\vec{g_j} = \Delta g_{j_x}\vec{u_x} + \Delta g_{j_y}\vec{u_y}$ are known in the base $\mathcal{B}$ for two non-collinear crystalline wave vectors (only valid for mono-crystalline samples A 7), then the strain deformation tensor can be deduced by calculating first the unstrained matrix G and the variation of the crystalline wave vectors matrix ΔG. Then, under assumptions A 4 and A 5, the deformation gradient tensor ∇u is estimated as the following with I_d representing the identity matrix (see annexe D in [4] and equation (30) in [5]).

$$G_{\text{uns}} = \begin{bmatrix} g_{1_x\,\text{uns}} & g_{1_y\,\text{uns}} \\ g_{2_x\,\text{uns}} & g_{2_y\,\text{uns}} \end{bmatrix}$$

$$\Delta G = \begin{bmatrix} \Delta g_{1_x} & \Delta g_{1_y} \\ \Delta g_{2_x} & \Delta g_{2_y} \end{bmatrix} \tag{23}$$

$$G = G_{\text{uns}} + \Delta G = \begin{bmatrix} g_{1_x\,\text{uns}} + \Delta g_{1_x} & g_{1_y\,\text{uns}} + \Delta g_{1_y} \\ g_{2_x\,\text{uns}} + \Delta g_{2_x} & g_{2_y\,\text{uns}} + \Delta g_{2_y} \end{bmatrix}$$

$$\nabla u = (G^T)^{-1}G_{\text{uns}}{}^T - I_d$$

<u>Source</u>: [4, 5]

<u>Ref by</u>: T 3, DD 1, IM 3, IM 5

5.2.5 Instance Models

IM 1 <mark>**Simulate the SMH on a reference to determine $\vec{q_j}$ for each $\vec{g_j}^M$**</mark>

- **Input**: $I_{SMH_{\text{exp}}}, I_{C_{\text{ref}}}, p$

- **Output**: $\widetilde{I}_{SMH_{\text{exp}}}, \widetilde{I}_{SMH_{\text{sim}}}, \overrightarrow{q_{n_j,m_j}}, \overrightarrow{g_j}^{M_{\text{ref}}}$

- **Description**: Considering that $I_{C_{\text{ref}}}$ represents a 2D array of the sample mono crys-talline lattice (A 6, A 7), the STEM Moiré hologram $I_{SMH_{\text{sim}}}$ with a scanning grid periodicity p and respecting the assumptions,A 1, A 2, A 3, is simulated to compare its Fourier transform $\widetilde{I}_{SMH_{\text{sim}}}$ manually to $\widetilde{I}_{SMH_{\text{exp}}}$ (the Fourier transform of the experimental STEM Moiré hologram $I_{SMH_{\text{exp}}}$). Using DD 2, the Fourier transform of the simulated STEM Moiré $\widetilde{I}_{SMH_{\text{sim}}}$ hologram is calculated using eq. (20):

$$\forall \vec{\nu} \in \Gamma, \widetilde{I}_{SMH_{\text{sim}}}(\vec{\nu}) = \frac{1}{p^2} \sum_{\vec{q} \in Q_{lim}} \widetilde{I}_{C_{\text{ref}}}(\vec{\nu} - \frac{\vec{q}}{p}) \tag{24}$$

  N_{lim} in Q_{lim} is set with respect to the highest spatial frequency resolved in $I_{C_{\text{ref}}}$ such that $\forall j \in [-j_{\text{lim}}, j_{\text{lim}}]$, $\mathcal{C}(\max(||\overrightarrow{g_j}^{C_{\text{ref}}}||) \times p) = N_{\text{lim}}$ where $\mathcal{C}$ is the ceiling function.

- **Source**: [6]

- **Ref by**: IM 4, IM 5, DD 2

[

  Extraction q and g|Details on the extraction of $\overrightarrow{q_{n_j,m_j}}$ and $\overrightarrow{g_j}^{M_{ref}}$
  For the moment, the extraction of $\overrightarrow{q_{n_j,m_j}}$ for a specific $\overrightarrow{g_j}^{M_{\text{ref}}}$ is manually done by the user by looking to the results ofIM 1 transforming the $\overrightarrow{g_j}^{C_{\text{ref}}}$ into $\overrightarrow{g_j}^{M_{\text{ref}}}$ as the following:

$$\overrightarrow{g_j}^{C_{\text{ref}}} - \overrightarrow{q_{n_j,m_j}} \times p = \overrightarrow{g_j}^{M_{\text{ref}}} \tag{25}$$

Equation (25) comes from eq. (22) by restraining SMH_{sim} in Γ. Identifying the frequency component, the following condition has to be respected:

$$(\overrightarrow{g_j}^{C_{ref}} - \overrightarrow{q} \times p) \in \Gamma$$

Since $\Gamma = [-\frac{1}{2p}, \frac{1}{2p}]^2$, there is only one possible $\overrightarrow{q} \times p$ vector that transform $\overrightarrow{g_j}^{C_{ref}}$ in Γ. Naming the only option $\overrightarrow{q_{n_j,m_j}}$ and the result of the transformation $\overrightarrow{g_j}^{M_{ref}}$ (as the Moiré wave vector), equation eq. (25) can be deduced. By choosing a Moiré wave vector in IM 2 $\overrightarrow{g_j}^{M_{ref}}$, the user selects the only possible $\overrightarrow{q_{n_j,m_j}}$ that is going to used in IM 4.

IM 2 **GPA on a selected Moiré wave vector from $I_{SMH_{exp}}$**

- **Input**: $\widetilde{I}_{SMH_{\text{exp}}}, M_j$

- **Output**: $P_{\Delta\overrightarrow{g_j}^{M_{\text{exp}}}}(\vec{r}), \overrightarrow{g_j}^{M_{\text{exp}}}, \Delta\overrightarrow{g_j}^{M_{\text{exp}}}(\vec{r})$

- **Description**: Applying DD 1 and using assumption A 1, $I_{SMH_{exp}}$ can be interpreted as follows

$$\forall \vec{r} \in \mathbb{I}, \ I_{SMH_{\exp}} = \sum_{j=-j_{\lim}}^{j=+j_{\lim}} A_j e^{i(\overrightarrow{g_j}^{M_{\exp}} \cdot \vec{r} + P_{\Delta \overrightarrow{g_j}^{M_{\exp}}})} \tag{26}$$

Applying GPA (T 2) under the assumptions A 4 and A 5, $P_{\Delta \overrightarrow{g_j}^{M_{\exp}}}$ is extracted using a mask M_j centred around $(g_{j_x}{}^{M_{\exp}}, g_{j_y}{}^{Mexp}) = \overrightarrow{g_j}^{M_{\exp}}$ with $\epsilon \in \mathbb{R}$ such that

$$\forall \nu \in \Gamma, M_j(\nu) = \begin{cases} 1 & \text{for } ||\vec{\nu} - \overrightarrow{g_j}^{M_{\exp}}|| \leq \epsilon \ / \ \forall \ l \neq j, \ ||\vec{\nu} - \overrightarrow{g_l}^{M_{\exp}}|| \geq \epsilon \\ 0 \end{cases} \tag{27}$$

Finally considering $M_j \widetilde{I}_{SMH_{\exp}}$ the masked Fourier transform of $I_{SMH_{\exp}}$,

$$\forall \vec{r} \in \mathbb{I}, \ P_{\Delta \overrightarrow{g_j}^{M_{\exp}}}(\vec{r}) = arg(\mathcal{FT}^{-1}[M_j \widetilde{I}_{SMH_{\exp}}])(\vec{r}) \tag{28}$$

Finally the gradient of the $P_{\Delta \overrightarrow{g_j}^{\exp}}(\vec{r})$ is calculated to extract $\Delta \overrightarrow{g_j}^{\exp}(\vec{r})$.

$$\forall \vec{r} \in \mathbb{I}, \ \nabla P_{\Delta \overrightarrow{g_j}^{M_{\exp}}}(\vec{r}) = 2\pi \Delta \overrightarrow{g_j}^{M_{\exp}}(\vec{r}) \tag{29}$$

- **Source**: [4]

- **Ref by**: IM 3, IM 5, DD 1, T 2, DD 2

IM 3 <mark>Determine an unstrained area in the geometric phase image</mark>

- **Input**: $\Delta \overrightarrow{g_j}^{M_{\exp}}(\vec{r}), U, \overrightarrow{g_j}^{M_{\exp}}$

- **Output**: $\overrightarrow{g_j}{}_{\mathrm{uns}}^{M_{\exp}}, \Delta \overrightarrow{g_j}{}_{\mathrm{cor}}^{M_{\exp}}(\vec{r})$

- **Description**: From DD 1 and IM 2, $\forall \vec{r} \in \mathbb{I}, \ \nabla P_{\Delta \overrightarrow{g_j}^{M_{\exp}}}(\vec{r}) = 2\pi \Delta \overrightarrow{g_j}^{M_{\exp}}(\vec{r})$. An area $U \in \mathbb{I}$ of $\Delta \overrightarrow{g_j}^{M_{\exp}}$ is set by the user as an unstrained reference. Therefore, $\Delta \overrightarrow{g_j}^{M_{\exp}}$ is set to $\vec{0}$ in U by correcting it with the vector $\overrightarrow{g_j}{}_{\mathrm{cor}}^{M_{\exp}}$. The operation can be formalized as follows with $card(U)$ representing the cardinality of the set U:

$$\forall \vec{r} \in U, \ \exists ! \ \overrightarrow{g_j}{}_{\mathrm{cor}}^{M_{\exp}} \ | \ R = \sum_{\vec{r} \in U} ||\Delta \overrightarrow{g_j}^{M_{\exp}}(\vec{r}) - \overrightarrow{g_j}{}_{\mathrm{cor}}^{M_{\exp}}||^2 \wedge \frac{dR}{d \overrightarrow{g_j}{}_{\mathrm{cor}}^{M_{\exp}}} = \vec{0} \tag{30}$$

The correction must be applied on the entire image $\mathbb{I}$ to get $\Delta \overrightarrow{g_j}{}_{\mathrm{cor}}^{M_{\exp}}$ and on $\overrightarrow{g_j}^{M_{\exp}}$ to get its corrected unstrained state $\overrightarrow{g_j}{}_{\mathrm{uns}}^{M_{\exp}}$.

$$\begin{aligned} \overrightarrow{g_j}{}_{\mathrm{uns}}^{M_{\exp}} &= \overrightarrow{g_j}^{M_{\exp}} - \overrightarrow{g_j}{}_{\mathrm{cor}}^{M_{\exp}} \\ \forall \vec{r} \in \mathbb{I}, \ \Delta \overrightarrow{g_j}{}_{\mathrm{cor}}^{M_{\exp}}(\vec{r}) &= \Delta \overrightarrow{g_j}^{M_{\exp}}(\vec{r}) - \overrightarrow{g_j}{}_{\mathrm{cor}}^{M_{\exp}} \end{aligned} \tag{31}$$

- **Source**: [4]

– **Ref by**: IM [2], DD [1], DD [3]

IM 4 **Convert the Moiré wave vector into the Crystalline wave vector**

– **Input**: $\overrightarrow{g_j}\,_{\text{uns}}^{M_{\exp}}, \Delta\overrightarrow{g_j}\,_{\text{cor}}^{M_{\exp}}(\vec{r}), \overrightarrow{q_{n_j,m_j}}, p$

– **Output**: $\Delta\overrightarrow{g_j}^{C_{exp}}(\vec{r}), \overrightarrow{g_j}\,_{uns}^{C_{exp}}$

– **Description**: The conversion is a basic affine vectorial transformation and is high-lighted in eq. (32).

$$\forall \vec{r} \in \mathbb{I}, \quad \begin{cases} \overrightarrow{g_j}\,_{\text{uns}}^{C_{\exp}} = \overrightarrow{g_j}\,_{\text{uns}}^{M_{\exp}} + p \times \overrightarrow{q_{n_j,m_j}} \\ \Delta\overrightarrow{g_j}^{C_{\exp}}(\vec{r}) = \Delta\overrightarrow{g_j}\,_{\text{cor}}^{M_{\exp}}(\vec{r}) + p \times \overrightarrow{q_{n_j,m_j}} \end{cases} \tag{32}$$

– **Source**: [6]

– **Ref by**: IM [1], IM [2], IM [3], DD [2], DD [3], DD [1]

IM 5 **Strain calculation using 2 non-crystalline wave vectors**

– **Input**: $g_{1_{\text{uns}_x}}^{C_{\exp}}, g_{1_{\text{uns}_y}}^{C_{\exp}}, g_{2_{\text{uns}_x}}^{C_{\exp}}, g_{2_{\text{uns}_y}}^{C_{\exp}}, \Delta g_{1_x}^{C_{\exp}}(\vec{r}), \Delta g_{1_y}^{C_{\exp}}(\vec{r}), \Delta g_{2_x}^{C_{\exp}}(\vec{r}), \Delta g_{2_y}^{C_{\exp}}(\vec{r})$

– **Output**: $\varepsilon_{xx}^{\exp}(\vec{r}), \varepsilon_{xy}^{\exp}(\vec{r}), \varepsilon_{yy}^{\exp}(\vec{r}), \omega_{xy}^{\exp}(\vec{r}), I_{\varepsilon_{xx}^{\exp}}, I_{\varepsilon_{xy}^{\exp}}, I_{\varepsilon_{yy}^{\exp}}, I_{\omega_{xy}^{\exp}}$

– **Description**: Applying DD [3] and T [3], the matrices $G_{\text{uns}}^{\exp}$ and $\Delta G^{\exp}$ are formed to calculate the deformation gradient tensor $\nabla u^{\exp}$ on each pixel as the following:

$$\forall \vec{r} \in \mathbb{I}, \ G_{\text{uns}}^{\exp} = \begin{bmatrix} g_{1_{\text{uns}_x}}^{C_{\exp}} & g_{2_{\text{uns}_x}}^{C_{\exp}} \\ g_{2_{\text{uns}_x}}^{C_{\exp}} & g_{2_{\text{uns}_y}}^{C_{\exp}} \end{bmatrix}$$

$$\forall \vec{r} \in \mathbb{I}, \ \Delta G^{\exp}(\vec{r}) = \begin{bmatrix} \Delta g_{1_x}^{C_{\exp}}(\vec{r}) & \Delta g_{1_y}^{C_{\exp}}(\vec{r}) \\ \Delta g_{2_x}^{C_{\exp}}(\vec{r}) & \Delta g_{2_y}^{C_{\exp}}(\vec{r}) \end{bmatrix} \tag{33}$$

$$\forall \vec{r} \in \mathbb{I}, \ G^{\exp}(\vec{r}) = G_{\text{uns}}^{\exp} + \Delta G^{\exp}(\vec{r})$$

$$\forall \vec{r} \in \mathbb{I}, \ \nabla u^{\exp}(\vec{r}) = (G^{\exp}(\vec{r})^T)^{-1} G_{\text{uns}}^{\exp T} - I_d$$

Then, the rotation $\omega^{\exp}$ and strain $\varepsilon^{\exp}$ tensors are determined on each pixel as follows:

$$\forall \vec{r} \in \mathbb{I}, \ \nabla u^{\exp}(\vec{r}) = \varepsilon^{\exp}(\vec{r}) + \omega^{\exp}(\vec{r})$$

$$\forall \vec{r} \in \mathbb{I}, \ \varepsilon^{\exp}(\vec{r}) = \begin{bmatrix} \varepsilon_{xx^{\exp}}(\vec{r}) & \varepsilon_{xy^{\exp}}(\vec{r}) \\ \varepsilon_{xy^{\exp}}(\vec{r}) & \varepsilon_{yy^{\exp}}(\vec{r}) \end{bmatrix}$$

$$\forall \vec{r} \in \mathbb{I}, \ \omega^{\exp}(\vec{r}) = \begin{bmatrix} 0 & \omega_{xy^{\exp}}(\vec{r}) \\ -\omega_{xy^{\exp}}(\vec{r}) & 0 \end{bmatrix} \tag{34}$$

$$\forall \vec{r} \in \mathbb{I}, \ \varepsilon^{\exp}(\vec{r}) = \frac{1}{2}(\nabla u^{\exp}(\vec{r}) + (\nabla u^{\exp}(\vec{r}))^T)$$

$$\forall \vec{r} \in \mathbb{I}, \ \omega^{\exp}(\vec{r}) = \frac{1}{2}(\nabla u^{\exp}(\vec{r}) - (\nabla u^{\exp}(\vec{r}))^T)$$

The data are finally displayed in form of 2D arrays, $I_{\varepsilon_{xx}}^{\mathrm{exp}}, I_{\varepsilon_{xy}}^{\mathrm{exp}}, I_{\varepsilon_{yy}}^{\mathrm{exp}}, I_{\omega_{xy}}^{\mathrm{exp}}$.

– **Source**: [4, 5]

– **Ref by**: IM 4, DD 3, T 3

5.2.6 Data Constraints

DC 1 U should be the same in both $\Delta\overrightarrow{g_j}^{M_{\mathrm{exp}}}$ with $j = \{1, 2\}$ in IM 3.

DC 2 The pixel size p should be strictly positive ($p > 0$).

DC 3 Both $I_{C_{\mathrm{ref}}}$ and $I_{SMH_{\mathrm{exp}}}$ can be dm3 files.

DC 4 A typical image (2D array $I_{C_{\mathrm{ref}}}$ or $I_{SMH_{\mathrm{exp}}}$) is composed of 2048×2048 pixels (size of the 2D array $I_{C_{\mathrm{ref}}}$ or $I_{SMH_{\mathrm{exp}}}$). There is no limit in the size of the data from the theoretical point of view, however the computing power to perform the calculations is not infinite. Therefore, it is recommended to use images up to a size of 2048×2048 pixels.

5.2.7 Properties of a Correct Solution

The correctness of the solution must be judged by the user him/herself based on the knowledge of the sample analysed.

6 Requirements

This section provides the functional requirements, the tasks that the software is expected to complete, and the nonfunctional requirements, the qualities that the software is expected to exhibit.

6.1 Functional Requirements

R 1 Provide an environment for the user to input $I_{SMH_{\mathrm{exp}}}$, p and $I_{C_{\mathrm{ref}}}$ (IM 1).

R 2 Verify the format of the inputs $I_{SMH_{\mathrm{exp}}}$ and $I_{C_{\mathrm{ref}}}$ to be 2D arrays composed of real numbers and verify p to be a real number strictly positive (IM 1).

R 3 Output $\widetilde{I}_{SMH_{\mathrm{exp}}}, \widetilde{I}_{SMH_{\mathrm{sim}}}$ (IM 1).

R 4 Display to the user $\widetilde{I}_{SMH_{\mathrm{exp}}}$ and $\widetilde{I}_{SMH_{\mathrm{sim}}}$ to allow the user to determine natural integers values n_j and m_j from $\overrightarrow{q_{n_j, m_j}}$ for each $\overrightarrow{g_j}^{M_{\mathrm{ref}}}$ (IM 1).

R 5 Provide an environment for the user to input M_j for each $\overrightarrow{g_j}^{M_{\mathrm{exp}}}$ with $j = \{1, 2\}$ on $\widetilde{I}_{SMH_{\mathrm{exp}}}$ (IM 2).

R 6 Verify both M_j inputs with $j = \{1,2\}$ to be different and to be 2D arrays of real numbers with the same dimensions than I_{SMH_exp} (IM 2).

R 7 Output both $P_{\Delta \overrightarrow{g_j}^{M_\mathrm{exp}}}$ and $\overrightarrow{g_j}^{M_\mathrm{exp}}$ with $j = \{1,2\}$ (IM 2).

R 8 Display both $\Delta \overrightarrow{g_j}^{M_\mathrm{exp}}$ with $j = \{1,2\}$ and provide an environment for the user to input U (IM 3).

R 9 Verify the input U to be a 2D array of real numbers with a smaller dimensions than I_{SMH_exp} (IM 3).

R 10 Output both $\overrightarrow{g_j}^{M_\mathrm{exp}}_\mathrm{uns}$ and $\Delta \overrightarrow{g_j}^{M_\mathrm{exp}}_\mathrm{cor}$ with $j = \{1,2\}$ (IM 3).

R 11 Provide an environment to the user to input the natural integers values n_j and m_j from $\overrightarrow{q_{n_j,m_j}}$ with $j = \{1,2\}$ (IM 4).

R 12 Output both $\Delta \overrightarrow{g_j}^{C_\mathrm{exp}}$ and both $\overrightarrow{g_j}^{C_\mathrm{exp}}_\mathrm{uns}$ with $j = \{1,2\}$ (IM 4).

R 13 Output $\varepsilon_{xx}^\mathrm{exp}, \varepsilon_{xy}^\mathrm{exp}, \varepsilon_{yy}^\mathrm{exp}, \omega_{xy}^\mathrm{exp}$ on each element of the array to form $I_{\varepsilon_{xx}^\mathrm{exp}}, I_{\varepsilon_{xy}^\mathrm{exp}}, I_{\varepsilon_{yy}^\mathrm{exp}}, I_{\omega_{xy}^\mathrm{exp}}$ (IM 5).

R 14 Display to the user $I_{\varepsilon_{xx}^\mathrm{exp}}, I_{\varepsilon_{xy}^\mathrm{exp}}, I_{\varepsilon_{yy}^\mathrm{exp}}, I_{\omega_{xy}^\mathrm{exp}}$ (IM 5).

6.2   Nonfunctional Requirements

NR 1 The software shall be reproducible on most used operating systems (Linux, Mac, Windows). The same raw data should show the same (or reasonably close to) results on the different operating systems.

NR 2 The software shall run on a modern desktop computer with at minimum a decent x86-CPU and a few GB of RAM.

NR 3 The data display shall be readable by the user (standard font, standard font size, standard organisation of display, standard colors).

NR 4 All environments expecting an input from the user shall be accessible and executable quickly (in a few seconds time frame).

NR 5 The user shall be able to extract the final data in text, csv or png format.

NR 6 The STEM Moiré GPA software shall be able to recover from a crash by allowing the user to resume the processing from a certain step.

NR 7 When starting the STEM Moiré GPA software, the user should be prompted to start a new processing or to resume an already existing one.

NR 8 The precision on the final results from STEM Moiré GPA software should be limited only by the quality of the initial SMH_exp and by the user inputs (LC 4).

NR 9 The inaccuracy of the STEM Moiré GPA software should not be greater than the precision detailed in NR 8.

7 Likely Changes (or Possible Changes)

LC 1 The determination of $\overrightarrow{q_{n_j,m_j}}$ for a specific $\overrightarrow{g_j}^{M_{\mathrm{ref}}}$ in IM 1 could be done automatically by the software. Nevertheless, the notion of "spatial frequency overlap" needs to be introduced and will complexify STEM Moiré GPA software. A decision has to be made between the potential simplification of the user experience and the time needed to implement the simplification.

LC 2 In T 2, the argument component in eq. (9) has an important constraint to output values between $[0; 2\pi[$ only. Therefore, the phase is said to be "wrapped" and observe a discontinuity at the value 2π. Phase unwrapping method needs to be implemented to process the data correctly. While initially considered as a lower level of implementation, various different phase unwrapping algorithms exist with different performance. Since accuracy and precision have been identified as a non-functional requirement, the unwrapping model would be considered to be added in the SRS document.

LC 3 The effect of the detector system such as gain non-uniformity, frequency cut-off, and distortions could be corrected to improve the accuracy of STEM Moiré GPA software. Those aspect would be considered to be added in STEM Moiré GPA software.

LC 4 A method to estimate the precision based on the quality of $I_{SMH_{exp}}$ and the user inputs will be added. If the measured precision on the final data is greater than the estimated one, the software is considered to be not precise.

8 Traceability Matrices and Graphs

The traceability matrices relate the interactions between different elements of the STEM Moiré GPA software. If one element from the column is modified, the section in the horizontal line with a cell crossed, have to be also changed. The traceability matrices are described below:

- Table 2 is showing the dependencies between the theoretical models, the data definitions and the instance models. Since STEM Moiré GPA software is mostly sequential, most dependencies are related to the input/output sequences. Only DD 1 is not following the input/output dependence and is involved in all other sections. Since the definition of strain in the crystalline lattice is defined in DD 1, a strong relation with all sections of STEM Moiré GPA software is indeed expected.

- Table 3 is highlighting the dependencies of the theoretical models, the data definitions and the instance models with respect to the assumptions. Two families affecting their respective sections can be observed:

    - Assumptions related to the sample A 4, A 5, A 6, A 7.
    - Assumptions related to the microscope A 1, A 2, A 3.

The assumptions were used to cover a certain variety of sample and to not be sensitive to different microscopes. However for dedicated applications, some of these assumptions can be removed.

— Table 4 is showing the dependencies between the instance models and the requirements. The sequential structure of STEM Moiré GPA is again visible here. IM 1 and IM 2 are the key elements of the software in which heavy calculations and multiple interactions with the users are performed. The high number of related requirements can be explained by the complexity factor.

	T 1	T 2	T 3	DD 1	DD 2	DD 3	IM 1	IM 2	IM 3	IM 4	IM 5
T 1											
T 2											
T 3											
DD 1		X									
DD 2	X			X							
DD 3				X							
IM 1	X			X	X						
IM 2		X		X	X		X				
IM 3				X		X		X			
IM 4	X			X	X		X		X		
IM 5			X	X		X				X	

Table 2: Traceability Matrix for the theoertical models TM, the data definitions DD and the instance models IM

	A 1	A 2	A 3	A 4	A 5	A 6	A 7
T 1							
T 2							
T 3				X	X		
DD 1				X	X		X
DD 2	X	X	X				
DD 3				X	X		X
IM 1	X	X	X			X	X
IM 2	X			X	X		
IM 3							
IM 4							
IM 5				X	X		

Table 3: Traceability Matrix linking the assumptions to the theoertical models TM, the data definitions DD and the instance models IM

21

	IM 1	IM 2	IM 3	IM 4	IM 5	R 1	R 2	R 3	R 4	R 5	R 6	R 7	R 8	R 9	R 10	R 11	R 12	R 13	R 14
IM 1						X	X	X											
IM 2	X					X	X	X	X	X		X	X						
IM 3		X										X	X		X				
IM 4	X		X			X			X				X			X	X	X	
IM 5				X													X	X	X
R 1	X	X																	
R 2	X	X				X													
R 3	X	X				X													
R 4	X	X				X		X											
R 5		X					X	X											
R 6		X								X									
R 7		X								X									
R 8		X	X						X			X							
R 9				X									X						
R 10				X									X						
R 11	X			X															
R 12				X												X			
R 13					X												X		
R 14					X													X	

Table 4: Traceability Matrix for the instance models IM and the requirements R

References

[1] W. S. Smith and L. Lai, "A new requirements template for scientific computing," in *Proceedings of the First International Workshop on Situational Requirements Engineering Processes – Methods, Techniques and Tools to Support Situation-Specific Requirements Engineering Processes, SREP'05* (J. Ralyté, P. Àgerfalk, and N. Kraiem, eds.), (Paris, France), pp. 107–121, In conjunction with 13th IEEE International Requirements Engineering Conference, 2005.

[2] W. S. Smith, L. Lai, and R. Khedri, "Requirements analysis for engineering computation: A systematic approach for improving software reliability," *Reliable Computing, Special Issue on Reliable Engineering Computation*, vol. 13, pp. 83–107, February 2007.

[3] R. C. Gonzalez and R. E. Woods, *Digital Image Processing.* Boston, MA, USA: Addison-Wesley Longman Publishing Co., Inc., 2nd ed., 1992.

[4] M. Hÿtch, E. Snoeck, and R. Kilaas, "Quantitative measurement of displacement and strain fields from HREM micrographs," *Ultramicroscopy*, vol. 74, pp. 131–146, aug 1998.

[5] J. Rouvière and E. Sarigiannidou, "Theoretical discussions on the geometrical phase analysis," *Ultramicroscopy*, vol. 106, pp. 1–17, dec 2005.

[6] A. Pofelski, S. Woo, B. H. Le, X. Liu, S. Zhao, W. Mi, S. Löffler, and G. Botton, "2d strain mapping using stem moiré interferometry and geometrical phase analysis." in review in Ultramicroscopy, May 2017.